

Micro- and nanoelectronics. Condensed matter physics  
Микро- и нанoeлектроника. Физика конденсированного состояния

UDC 544.225

<https://doi.org/10.32362/2500-316X-2025-13-4-47-54>

EDN STUTJW



## RESEARCH ARTICLE

## *Ab initio* calculations of the electronic structure of CeI<sub>3</sub> monolayer

Elizaveta T. Mirzoeva,  
Andrey V. Kudryavtsev @

MIREA – Russian Technological University, Moscow, 119454 Russia

@ Corresponding author, e-mail: kudryavtsev\_a@mirea.ru

• Submitted: 15.01.2025 • Revised: 14.02.2025 • Accepted: 15.05.2025

**Abstract**

**Objectives.** In comparison with three-dimensional structures, two-dimensional (2D) magnetic materials are promising for use in spintronics and magnetic storage devices due to their exceptional characteristics and qualitatively different physical properties. Theoretical studies into 2D magnetic structures pave the way for the development of new compounds based on experimental data. In this work, we carry out a theoretical calculation of the electronic structure of a CeI<sub>3</sub> 2D-magnetic material, taking into account the Hubbard repulsion at the site, the partial density of electronic states (DOS), and the distribution of spin and charge densities.

**Methods.** Calculations of the electronic structure of the CeI<sub>3</sub> monolayer were performed using density functional theory (DFT) and the Hubbard U scheme in the VASP software environment. The Dudarev method was used to account for the Hubbard correction.

**Results.** The calculated densities of the electronic states and the bandgap values for the ferro- and antiferromagnetic configurations of the material were found to be 1.98 and 2.08 eV, respectively. To assess the influence of correlation effects, the DOS was calculated both with and without the Hubbard correction. It was determined that the system in the ground magnetic state exhibits an antiferromagnetic ordering of the spin subsystem. The difference in the total energies of the antiferro- and ferromagnetic configurations was 2.8 meV per formula unit.

**Conclusions.** The calculations based on the Hubbard correction clearly demonstrated the presence of a bandgap, which is typical of semiconductor materials. The obtained bandgaps for the ferromagnetic and antiferromagnetic configurations of the system belong to the visible light range, which offers the opportunity of using 2D CeI<sub>3</sub> as a luminescent material in devices with a magnetically controlled emission. To assess the influence of correlation effects, the DOS was calculated both with and without the Hubbard correction. The obtained results agree with those obtained in experimental studies of cerium compounds. The consideration of correlation effects and spin polarization in the presented calculations forms the basis for further research into the magnetic properties of the CeI<sub>3</sub> monolayer for technological applications in the field of 2D magnetism.

**Keywords:** two-dimensional magnetism, 2D magnetism, density functional theory, DFT, Hubbard correction, rare-earth metals, density of electronic states, luminescence

**For citation:** Mirzoeva E.T., Kudryavtsev A.V. *Ab initio* calculations of the electronic structure of  $\text{CeI}_3$  monolayer. *Russian Technological Journal*. 2025;13(4):47–54. <https://doi.org/10.32362/2500-316X-2025-13-4-47-54>, <https://www.elibrary.ru/STUTJW>

**Financial disclosure:** The authors have no financial or proprietary interest in any material or method mentioned.

The authors declare no conflicts of interest.

## НАУЧНАЯ СТАТЬЯ

# Первопринципный расчет электронной структуры монослоя $\text{CeI}_3$

Е.Т. Мирзоева,  
А.В. Кудрявцев<sup>@</sup>

МИРЭА – Российский технологический университет, Москва, 119454 Россия

<sup>@</sup> Автор для переписки, e-mail: kudryavtsev\_a@mirea.ru

• Поступила: 15.01.2025 • Доработана: 14.02.2025 • Принята к опубликованию: 15.05.2025

### Резюме

**Цели.** Двумерные магнетики, благодаря своим уникальным характеристикам и качественно новым физическим свойствам по сравнению с объемными структурами, обладают значительным потенциалом для применения в спинтронике и магнитных запоминающих устройствах. Теоретические исследования двумерных магнитных структур позволяют сузить область поиска новых соединений и дополнить экспериментальные данные. Целью данной работы является теоретический расчет электронной структуры двумерного магнетика  $\text{CeI}_3$ , включающий учет хаббардовского отталкивания на узле, расчет парциальной плотности электронных состояний и расчет распределения спиновых и зарядовых плотностей.

**Методы.** Расчеты электронной структуры монослоя  $\text{CeI}_3$  выполнены с использованием программного пакета VASP в рамках теории функционала плотности, а также в рамках теории функционала плотности с учетом поправки Хаббарда. Для учета поправки Хаббарда использовался метод Дударева.

**Результаты.** Рассчитаны энергетические плотности электронных состояний и величины запрещенных зон для ферро- и антиферромагнитной конфигураций материала, равные соответственно 1.98 и 2.08 эВ. Для оценки влияния корреляционных эффектов проведен расчет плотностей состояний как с учетом поправки Хаббарда, так и без него. Определено, что в основном магнитном состоянии система проявляет антиферромагнитное упорядочение спиновой подсистемы. Разница полных энергий с ферромагнитной конфигурацией составила 2.8 мэВ на формульную единицу.

**Выводы.** Учет поправки Хаббарда наглядно продемонстрировал наличие характерной для полупроводниковых материалов запрещенной зоны. Полученные ширины запрещенной зоны для ферромагнитной и антиферромагнитной конфигураций системы относятся к диапазону видимого света, что открывает возможности использования двумерного  $\text{CeI}_3$  в качестве люминесцентного материала в устройствах с магнитным управлением излучения. Представленные результаты согласуются с обобщенными результатами экспериментальных исследований соединений на основе церия. Учет корреляционных эффектов и поляризации по спину в представленных расчетах открывает горизонт для дальнейшего изучения магнитных свойств монослоя  $\text{CeI}_3$  для технологических применений в области двумерного магнетизма.

**Ключевые слова:** двумерный магнетизм, теория функционала плотности, поправка Хаббарда, редкоземельные металлы, плотность электронных состояний, люминесценция

**Для цитирования:** Мирзоева Е.Т., Кудрявцев А.В. Первопринципный расчет электронной структуры моно-слоя  $\text{CeI}_3$ . *Russian Technological Journal*. 2025;13(4):47–54. <https://doi.org/10.32362/2500-316X-2025-13-4-47-54>, <https://www.elibrary.ru/STUTJW>

**Прозрачность финансовой деятельности:** Авторы не имеют финансовой заинтересованности в представленных материалах или методах.

Авторы заявляют об отсутствии конфликта интересов.

## INTRODUCTION

Two-dimensional (2D) magnets represent a new class of low-dimensional materials. These materials exhibit a number of unique properties that are promising from the practical point of view. Thus, the magnetic anisotropy of such materials makes it possible to control the properties of a system by changing the direction of an external magnetic field [1]. Magnetic anisotropy is of great importance for 2D ferromagnetism in the sense of avoiding a random redistribution of spin states due to thermal fluctuations. Other important properties of systems based on 2D magnets include the magnetic proximity effect [2], the formation of skyrmions [3], the quantum anomalous Hall effect [4], giant magnetoresistance [5], etc.

In this regard, 2D magnets are promising materials for use in spintronics and magnetic memory devices [6–8]. Experimental studies have confirmed the presence of a long-range magnetic ordering in these materials [9, 10], although the Mermin–Wagner theorem states the impossibility of magnetic ordering in two-dimensional systems at temperatures above zero [11].

At present, the search for materials and compounds with a set of practically important properties is a pressing task. Bulk compounds can be studied both experimentally and theoretically; however, their 2D analogs may exhibit qualitatively different physical properties, which makes their experimental study challenging. In this regard, first-principles (*ab initio*) calculations of material structures are of particular interest. Another powerful theoretical tool comprises calculations using density functional theory (DFT).

In this paper, we carry out an *ab initio* calculation of the physical properties of 2D  $\text{CeI}_3$  with orthorhombic symmetry. Along with such 2D materials as transition metal dichalcogenides that have been sufficiently studied [12], new 2D compounds promising in terms of their luminescent properties are increasingly attracting attention. These include 2D materials based on rare-earth elements [13, 14]. The  $5d$ – $4f$  transitions in the Ce atom have a short lifetime of about 17 ns, which ensures a high luminescence efficiency [15]. The magnetic properties of 2D magnets are due to partially filled  $d$  and  $f$  electron shells. Thus, information on the magnetic properties of 2D  $\text{CeI}_3$  may pave the way not

only for its potential use in spintronics, but also for the creation of optical devices with the magnetic control of emission.

## CALCULATION PROCEDURE

The calculations were performed using Vienna *Ab initio* Simulation Package (*VASP*), a commercially available *ab initio* simulation package. *VASP* is a widely used package designed for calculations using DFT [16] to determine the properties of materials in the ground state (total energy, band structure, density of electronic states (DOS), phonon spectra, etc.) by solving the Kohn–Sham equations.

In the presented calculations, the exchange–correlation energy of electrons was approximated by the generalized gradient approximation using the Perdew–Burke–Ernzerhof functional [17]. Electron–ion interactions were described by the project augmented wave method [18]. To define the 2D structure under the three-dimensional (3D) boundary conditions, a 25 Å pseudovacuum space was added to eliminate the interaction between layers during unit cell translation. The plane wave basis cutoff energy was set to 320 eV. For integration over the Brillouin zone, a gamma-centered  $k$ -point grid of  $16 \times 16 \times 1$  was used for structure relaxation;  $20 \times 20 \times 1$ , for self-consistent calculation; and  $26 \times 26 \times 1$ , for DOS calculation. The crystal structure was relaxed until the total forces acting on each atom were less than 0.001 eV/Å. The relaxation of the electronic degrees of freedom was discontinued when the energy difference between two calculation iterations was less than  $10^{-6}$  eV. To account for the van der Waals forces, a semiclassical dispersion correction known as DFT-D3 with the Becke–Johnson damping function was used [19].

For rare-earth metals, account should be taken of the repulsion of localized (strongly correlated) electron shells  $d$  and  $f$ . To increase the accuracy of the sought parameters, the Hubbard repulsion (DFT+U) was taken into account. The DFT+U calculation implies the separation of localized  $d$  and  $f$  electrons, for which the Hubbard correction is considered, and delocalized  $s$  and  $p$  electrons. The Hubbard correction was taken into account using the Dudarev approach described in [20]:

$$E_{\text{DFT+U}} = E_{\text{DFT}} + \frac{U - J}{2} \times \sum_{\sigma} \left[ \left( \sum_{m_1} n_{m_1, m_2}^{\sigma} \right) - \left( \sum_{m_1, m_2} n_{m_1, m_2}^{\sigma} n_{m_2, m_1}^{\sigma} \right) \right], \quad (1)$$

where  $m_1$  and  $m_2$  are magnetic quantum numbers ( $m_1, m_2 = -3, -2, \dots, 3$  in the case of  $f$ -shell electrons);  $n_{m_1, m_2}^{\sigma}$  is the matrix element of the density matrix with spin  $\sigma$ ;  $U$  is the parameter characterizing the Coulomb repulsion at the site, which was taken to be 5.1 eV for the Ce 4*f* level; and  $J$  is the parameter characterizing the interstitial repulsion of  $d$  and  $f$  electrons [21, 22].

The first term of  $E_{\text{DFT}}$  is the energy of delocalized  $s$  and  $p$  electrons, which is conventionally calculated using DFT in the generalized gradient approximation. The second term takes into account the electron–electron interaction (Hubbard correction) for localized  $d$  and  $f$  electrons.

The crystal structure and the spin and charge densities were visualized using the *VESTA* software [23]. The data obtained by the DFT calculation were processed using the *VASP*KIT software [24].

## RESULTS AND DISCUSSION

In this paper, we calculated the energy densities of electronic states and the bandgap values for ferromagnetic (FM) and antiferromagnetic (AFM) configurations of the material, along with determination of the configuration with the minimum total energy. The unit cell of the CeI<sub>3</sub> monolayer contains two cerium atoms and six iodine atoms. The crystal structure is an orthorhombic with unit cell parameters of  $4.32 \times 9.98 \text{ \AA}$  and a pseudovacuum space of  $25 \text{ \AA}$  (Fig. 1). Cerium atoms are marked in yellow; iodine atoms are marked in violet. The model cell is outlined by a solid black line.

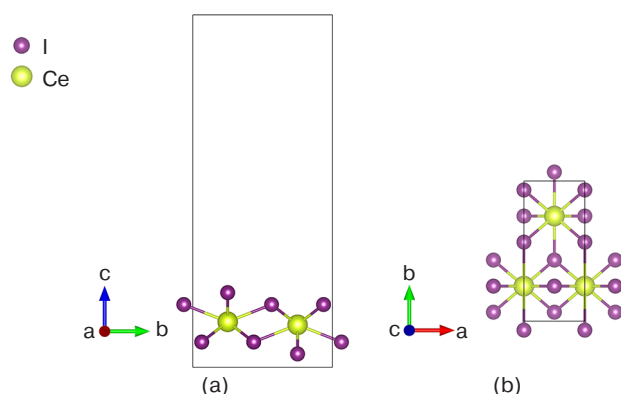


**Fig. 1.** CeI<sub>3</sub> monolayer: (a) side view; (b) top view

Figure 2 presents the dependencies of the partial densities and total DOS on energy for the FM configuration that were obtained using DFT without taking into account the Hubbard correction (DFT calculation).

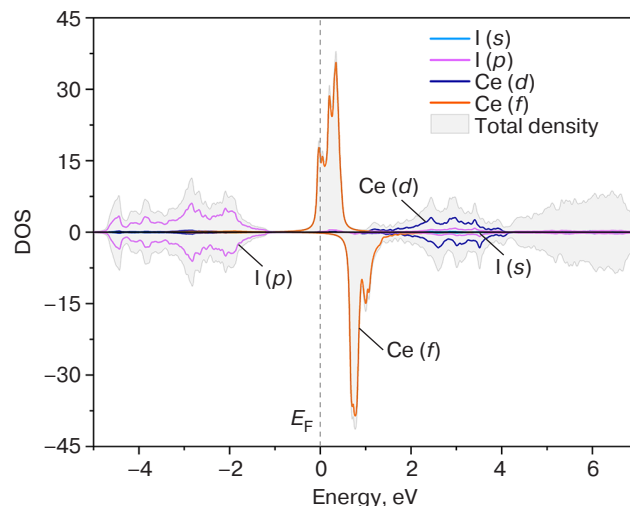


**Fig. 2.** DOS of the CeI<sub>3</sub> monolayer for the FM configuration (DFT calculation): total DOS (full pattern) and contributions of  $s$  states of iodine (blue),  $p$  states of iodine (purple),  $d$  states of cerium (deep blue), and  $f$  states of cerium (orange),  $E_F$  is the Fermi energy

The presented dependence of the DOS does not show a bandgap, which is characteristic of semiconductors, although 2D CeI<sub>3</sub> is presumably a semiconductor material. This discrepancy is due to incorrect consideration of the correlation effects for localized electrons of the outer shells of cerium using standard DFT. To solve this problem, Hubbard corrections were introduced by the Dudarev method. This method appears optimal for calculations.

It should be noted that the general structure of these dependencies is similar to that of the dependence of the DOS for a 3D CeI<sub>3</sub> crystal [25]. In that work, the valence band was formed by  $p$  states of iodine, the conduction band was formed by  $d$  states of cerium, and 4*f* states of cerium were located in the bandgap. However, the calculations [25] were carried out, as indicated above, for a 3D material, without taking correlation effects and spin polarization into account. These considerations impede further studies of magnetic properties, in contrast to the calculations presented in this article.

Figure 3 presents the dependencies of the densities of electronic states of the CeI<sub>3</sub> monolayer that were obtained using DFT and taking the Hubbard correction (DFT+U) into account. As expected, the material is a semiconductor with a bandgap of  $\sim 1.9 \text{ eV}$  between the  $p$  shells of iodine and the  $f$  shells of cerium. The obtained bandgap value agrees with that obtained in experimental studies of compounds of rare-earth elements, including cerium [26, 27].

Cerium is the first element in which occupied states appear on the  $f$  shell. This is confirmed by the presence of a corresponding peak in the valence band region. The general form of the DOS is characteristic of a ferri- or ferromagnetic structure with two spin subsystems that do not compensate each other completely.

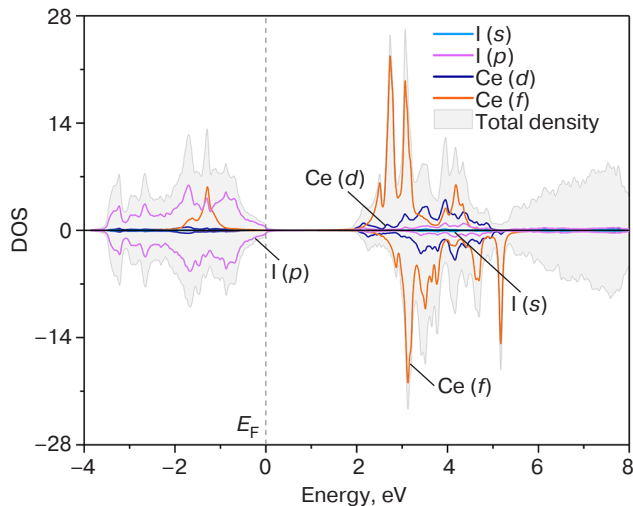


**Fig. 3.** DOS of the  $\text{CeI}_3$  monolayer taking the Hubbard correction into account (DFT+U calculation): total DOS (full pattern) and contributions of *s* states of iodine (blue), *p* states of iodine (purple), *d* states of cerium (deep blue), and *f* states of cerium (orange)

To calculate the AFM configuration, a structural supercell of  $2 \times 2$  unit cells was generated, which comprised 8 cerium atoms and 24 iodine atoms. In addition, the FM supercell was calculated for a comparative analysis and further determination of the type of magnetic ordering corresponding to the minimum total energy.

The DFT+U calculations gave the densities of electronic states (Fig. 4), the spin density distributions (Fig. 5) for the FM and AFM configurations, as well as the general form of the charge density distribution (Fig. 6).

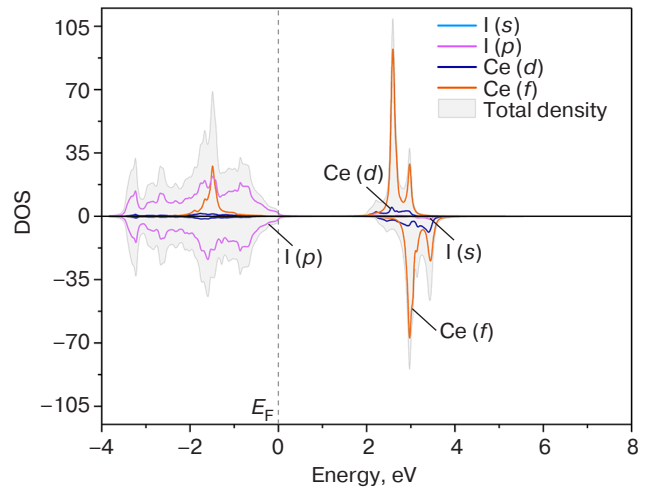
The presented dependencies of the DOS indicate that the energy bandgap width is about 2.08 and 1.98 eV for the AFM and FM configurations, respectively. The obtained values of the bandgap width correspond to the visible light range.

To determine the ground magnetic state, the difference between the total energies of the AFM and FM configurations should be found:

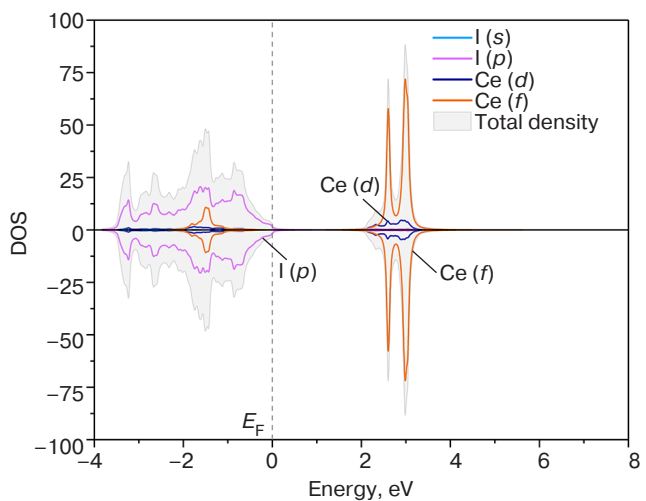
$$\Delta E = E_{\text{AFM}} - E_{\text{FM}} = -2.8 \text{ meV.} \quad (2)$$

The negative value indicates that, energetically, AFM is the most favorable configuration for the structure under study due to its lower energy. Different values of the total energy are explained by different contributions of the Coulomb repulsion between parallel and antiparallel spins of the outer shells of the system.

The spin density distributions for both configurations (Fig. 5) have the form of a dumbbell concentrated around the cerium atom with a nonzero magnetic moment in accordance with the assumed



(a)



(b)

**Fig. 4.** DOS of the  $\text{CeI}_3$  monolayer in the (a) FM and (b) AFM configurations: total DOS (full pattern) and contributions of *s* states of iodine (blue), *p* states of iodine (purple), *d* states of cerium (deep blue), and *f* states of cerium (orange)

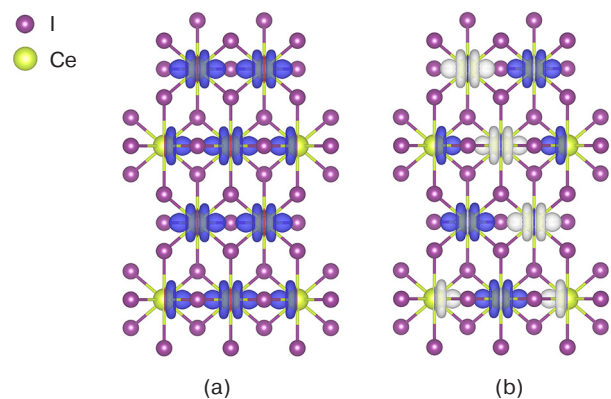


**Fig. 5.** Spin density distributions in the  $\text{CeI}_3$  supercell for the (a) FM and (b) AFM configurations on isosurfaces of  $\pm 0.0009 \text{ e}/\text{\AA}^3$  in the spin-up (blue) and spin-down (white) polarizations



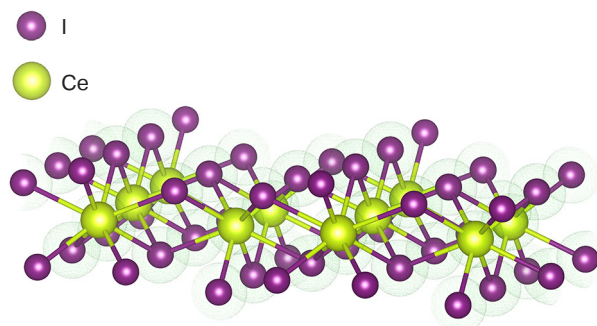


**Fig. 6.** Charge density distribution in the  $\text{CeI}_3$  supercell on the  $0.066 \text{ e}/\text{\AA}^3$  isosurface. Isosurfaces are shown in light green

form of the  $f$  shell orbitals. The charge density distribution (Fig. 6) indicates the concentration of the negative charge around the iodine atoms, which is due to the greater electronegativity of the halogen atoms. Such a shift in the charge density confirms a large contribution of covalence to the metal–halogen chemical bonds. The formation of covalent bonds between Ce–I pairs creates the possibility of superexchange interaction between neighboring Ce atoms.

## CONCLUSIONS

In this work, the *ab initio* calculation of the electronic structure of a new two-dimensional compound— $\text{CeI}_3$ —was performed using density functional theory. The calculation of the densities of electronic states taking the Hubbard correction into account clearly demonstrated

the presence of a bandgap, which is characteristic of semiconductor materials. The bandgap values for the FM and AFM configurations of the material were 1.98 and 2.08 eV, respectively. Such energy values belong to the visible light range, which offers the opportunity of using two-dimensional  $\text{CeI}_3$  as a luminescent material in devices with the magnetic control of emission. According to the calculations, the AFM configuration has a lower total energy, i.e., being the ground magnetic state of the structure. The difference between the total energies of the FM and AFM configurations (2.8 meV) is due to different contributions of the Coulomb repulsion between the parallel and antiparallel spins of the outer shells of the system. The presence of covalent polar bonds, which is clearly demonstrated by the charge density distribution, creates the possibility of superexchange interaction between neighboring cerium atoms. The obtained results form a basis for further research and technological applications of the  $\text{CeI}_3$  monolayer in the field of two-dimensional magnetism.

## ACKNOWLEDGMENTS

The calculations were performed using the equipment of the Center for the Collective Use of Computing Resources of the National Research Center “Kurchatov Institute.”

### Authors' contributions

**E.T. Mirzoeva**—performing calculations, processing results, writing the manuscript.

**A.V. Kudryavtsev**—performing calculations, discussing the results, writing the manuscript.

## REFERENCES

1. Tan H., Shan G., Zhang J. Prediction of novel two-dimensional room-temperature ferromagnetic rare-earth material –  $\text{GdB}_2\text{N}_2$  with large perpendicular magnetic anisotropy. *Mater. Today Phys.* 2022;24:100700. <https://doi.org/10.1016/j.mtphys.2022.100700>
2. Vobornik I., Manju U., Fujii J., Borgatti F., Torelli P., Krizmancic D., Hor Y.S., Cava R.J., Panaccione G. Magnetic proximity effect as a pathway to spintronic applications of topological insulators. *Nano Lett.* 2011;11(10):4079–4082. <https://doi.org/10.1021/nl201275q>
3. Heinze S., Von Bergmann K., Menzel M., et al. Spontaneous atomic-scale magnetic skyrmion lattice in two dimensions. *Nature Phys.* 2011;7(9):713–718. <https://doi.org/10.1038/nphys2045>
4. Zhang J., Zhao B., Yao Y., Yang Z. Robust quantum anomalous Hall effect in graphene-based van der Waals heterostructures. *Phys. Rev. B.* 2015;92(16):165418. <https://doi.org/10.1103/PhysRevB.92.165418>
5. Song T., Cai X., Tu M.W.Y., Zhang X., Huang B., Wilson N.P., Seyler K.L., Zhu L., Taniguchi T., Watanabe K., McGuire M.A., Cobden D.H., Xiao D., Yao W., Xu X. Giant tunneling magnetoresistance in spin-filter van der Waals heterostructures. *Science.* 2018;360(6394):1214–1218. <https://doi.org/10.1126/science.aar4851>
6. Wang Z., Sapkota D., Taniguchi T., Watanabe K., Mandrus D., Morpurgo A.F. Tunneling spin valves based on  $\text{Fe}_3\text{GeTe}_2/\text{hBN}/\text{Fe}_3\text{GeTe}_2$  van der Waals heterostructures. *Nano Lett.* 2018;18(7):4303–4308. <https://doi.org/10.1021/acs.nanolett.8b01278>
7. Ashton M., Gluhovic D., Sinnott S.B., Guo J., Stewart D.A., Hennig R.G. Two-dimensional intrinsic half metals with large spin gaps. *Nano Lett.* 2017;17(9):5251–5257. <https://doi.org/10.1021/acs.nanolett.7b01367>
8. Johansen Ø., Risinggård V., Sudbø A., Linder J., Brataas A. Current control of magnetism in two-dimensional  $\text{Fe}_3\text{GeTe}_2$ . *Phys. Rev. Lett.* 2019;122(21):217203. <https://doi.org/10.1103/PhysRevLett.122.217203>

9. Jiang X., Liu Q., Xing J., Liu N., Guo Y., Liu Z., Zhao J. Recent progress on 2D magnets: Fundamental mechanism, structural design and modification. *Appl. Phys. Rev.* 2021;8(3):031305. <https://doi.org/10.1063/5.0039979>
10. Tian S., Zhang J.-F., Li C., Ying T., Li S., Zhang X., Liu K., Lei H. Ferromagnetic van der Waals crystal  $\text{VI}_3$ . *Am. Chem. Soc.* 2019;141(13):5326–5333. <https://doi.org/10.1021/jacs.8b13584>
11. Mermin N.D., Wagner H. Absence of Ferromagnetism or Antiferromagnetism in One- or Two-Dimensional Isotropic Heisenberg Models. *Phys. Rev. Lett.* 1966;17(22):1133–1136. <https://doi.org/10.1103/PhysRevLett.17.1133>
12. Pimenov N.Yu., Lavrov S.D., Kudryavtsev A.V., Avdizhiyan A.Yu. Modeling of two-dimensional  $\text{MoxW}_{1-x}\text{S}_{2y}\text{Se}_{2(1-y)}$  alloy band structure. *Russian Technological Journal.* 2022;10(3):56–63. <https://doi.org/10.32362/2500-316X-2022-10-3-56-63>
13. Guo Q., Wang L., Yang L., et al. Spectra stable deep-blue light-emitting diodes based on cryolite-like cerium(III) halides with nanosecond d-f emission. *Sci. Adv.* 2022;8(50):eabq2148. <https://doi.org/10.1126/sciadv.abq2148>
14. Wang C., Liu X., She C., Li Y. Luminescence of  $\text{CeI}_3$  in organic solvents and its application in water detection. *Polyhedron.* 2021;196:115013. <https://doi.org/10.1016/j.poly.2020.115013>
15. Xie W., Hu F., Gong S., Peng L. Study the optical properties of  $\text{Cs}_3\text{CeI}_6$ : First-principles calculations. *AIP Advances.* 2024;14:015062. <https://doi.org/10.1063/5.0187100>
16. Kresse G., Furthmüller J. Efficiency of *ab initio* total energy calculations for metals and semiconductors using a plane-wave basis set. *Phys. Rev. B.* 1996;54(16):11169–11186. <https://doi.org/10.1103/PhysRevB.54.11169>
17. Constantin L.A., Perdew J.P., Pitarke J.M. Exchange–correlation hole of a generalized gradient approximation for solids and surfaces. *Phys. Rev. B.* 2009;79(7):075126. <https://doi.org/10.1103/PhysRevB.79.075126>
18. Kresse G., Joubert D. From ultrasoft pseudopotentials to the projector augmented-wave method, *Phys. Rev. B.* 1999;59(3):1758–1775. <https://doi.org/10.1103/PhysRevB.59.1758>
19. Grimme S., Ehrlich S., Goerigk L. Effect of the damping function in dispersion corrected density functional theory. *J. Comput. Chem.* 2011;32(7):1456–1465. <https://doi.org/10.1002/jcc.21759>
20. Dudarev S.L., Botton G.A., Savrasov S.Y., Humphreys C.J., Sutton A.P. Electron-energy-loss spectra and the structural stability of nickel oxide: An LSDA+*U* study. *Phys. Rev. B.* 1998;57(3):1505–1509. <https://doi.org/10.1103/PhysRevB.57.1505>
21. Sheng K., Chen Q., Yuan H., Wang Z. Monolayer  $\text{CeI}_2$ : An intrinsic room-temperature ferrovalley semiconductor. *Phys. Rev. B.* 2022;105(7):075304. <https://doi.org/10.1103/PhysRevB.105.075304>
22. Larson P., Lambrecht W.R.L., Chantis A., van Schilfgaarde M. Electronic structure of rare-earth nitrides using the LSDA+*U* approach: Importance of allowing 4*f* orbitals to break the cubic crystal symmetry. *Phys. Rev. B.* 2007;75(4):045114. <https://doi.org/10.1103/PhysRevB.75.045114>
23. Momma K., Izumi F. *VESTA*: a three-dimensional visualization system for electronic and structural analysis. *J. Appl. Cryst.* 2008;41:653–658. <https://doi.org/10.1107/S0021889808012016>
24. Wang V., Xu N., Liu J., Tang G., Geng W. VASPKIT: A user-friendly interface facilitating high-throughput computing and analysis using VASP code. *Comput. Phys. Commun.* 2021;267:108033. <https://doi.org/10.1016/j.cpc.2021.108033>
25. Chornodolskiy Ya.M., Karnaushenko V.O., Vistovskiy V.V., Syrotyuk S.V., Gektin A.V., Voloshinovskii A.S. Energy band structure peculiarities and luminescent parameters of  $\text{CeX}_3$  ( $\text{X} = \text{Cl}, \text{Br}, \text{I}$ ) crystals. *J. Lumin.* 2021;237:118147. <https://doi.org/10.1016/j.jlumin.2021.118147>
26. Birowosuto M.D., Dorenbos P. Novel  $\gamma$ - and X-ray scintillator research: on the emission wavelength, light yield and time response of  $\text{Ce}^{3+}$  doped halide scintillators. *Phys. Status Solidi A-Appl. Mater. Sci.* 2009;206(1):9–20. <https://doi.org/10.1002/pssa.200723669>
27. Dorenbos P. Lanthanide 4*f*-electron binding energies and the nephelauxetic effect in wide band gap compounds. *J. Lumin.* 2013;136:122–129. <https://doi.org/10.1016/j.jlumin.2012.11.030>

## About the Authors

**Elizaveta T. Mirzoeva**, Master Student, Institute for Advanced Technologies and Industrial Programming, MIREA – Russian Technological University (78, Vernadskogo pr., Moscow, 119454 Russia). E-mail: mirzoeva.elizaveta@gmail.ru. <https://orcid.org/0009-0003-4874-7015>

**Andrey V. Kudryavtsev**, Cand. Sci. (Phys.-Math.), Associate Professor, Researcher, Department of Nanoelectronics, Institute for Advanced Technologies and Industrial Programming, MIREA – Russian Technological University (78, Vernadskogo pr., Moscow, 119454 Russia). E-mail: kudryavcev\_a@mirea.ru. Scopus Author ID 55219889700, ResearcherID O-1457-2016, <https://orcid.org/0000-0002-2126-7404>

#### Об авторах

**Мирзоева Елизавета Теофиловна**, магистрант, Институт перспективных технологий и индустриального программирования, ФГБОУ ВО «МИРЭА – Российский технологический университет» (119454, Россия, Москва, пр-т Вернадского, д. 78). E-mail: mirzoeva.elizaveta@gmail.ru. <https://orcid.org/0009-0003-4874-7015>

**Кудрявцев Андрей Владимирович**, к.ф.-м.н., доцент, научный сотрудник, кафедра наноэлектроники, Институт перспективных технологий и индустриального программирования, ФГБОУ ВО «МИРЭА – Российский технологический университет» (119454, Россия, Москва, пр-т Вернадского, д. 78). E-mail: kudryavcev\_a@mirea.ru. Scopus Author ID 55219889700, ResearcherID O-1457-2016, <https://orcid.org/0000-0002-2126-7404>

*Translated from Russian into English by V. Glyanchenko*

*Edited for English language and spelling by Thomas A. Beavitt*